crystals

MDPI

Article

Small-Polaron Hopping and Low-Temperature (45–225 K) Photo-Induced Transient Absorption in Magnesium-Doped Lithium Niobate †

Simon Messerschmidt [1,‡], Andreas Krampf [1,‡], Laura Vittadello [1], Mirco Imlau [1,*], Tobias Nörenberg [2], Lukas M. Eng [2,3] and David Emin [4]

[1] School of Physics, Osnabrueck University, Barbarastraße 7, 49076 Osnabrueck, Germany; smesserschmi@uni-osnabrueck.de (S.M.); andreas.krampf@uni-osnabrueck.de (A.K.); laura.vittadello@uni-osnabrueck.de (L.V.)
[2] Institut für Angewandte Physik, TU Dresden, Nöthnitzerstr. 61, 01187 Dresden, Germany; tobias.noerenberg@tu-dresden.de (T.N.); lukas.eng@tu-dresden.de (L.M.E.)
[3] ct.qmat: Dresden-Würzburg Cluster of Excellence—EXC 2147, Technische Universität Dresden, 01069 Dresden, Germany
[4] Department of Physics and Astronomy, University of New Mexico, Albuquerque, NM 87131, USA; emin@unm.edu
* Correspondence: mirco.imlau@uni-osnabrueck.de
† Dedicated to the memory of Ortwin F. Schirmer (1937–2020).
‡ These authors contributed equally to this work.

Received: 20 August 2020; Accepted: 11 September 2020; Published: 14 September 2020

Abstract: A strongly temperature-dependent photo-induced transient absorption is measured in 6.5 mol% magnesium-doped lithium niobate at temperatures ranging from 45 K to 225 K. This phenomenon is interpreted as resulting from the generation and subsequent recombination of oppositely charged small polarons. Initial two-photon absorptions generate separated oppositely charged small polarons. The existence of these small polarons is monitored by the presence of their characteristic absorption. The strongly temperature-dependent decay of this absorption occurs as series of thermally assisted hops of small polarons that facilitate their merger and ultimate recombination. Our measurements span the high-temperature regime, where small-polaron jump rates are Arrhenius and strongly dependent on temperature, and the intermediate-temperature regime, where small-polaron jump rates are non-Arrhenius and weakly dependent on temperature. Distinctively, this model provides a good representation of our data with reasonable values of its two parameters: Arrhenius small-polaron hopping's activation energy and the material's characteristic phonon frequency.

Keywords: lithium niobate; small polaron hopping; transient absorption

1. Introduction

This paper is in memoriam of Ortwin Schirmer who throughout his long career pioneered the study of lithium niobate. Lithium niobate ($LiNbO_3$, LN) is widely employed in electro-, acousto- and nonlinear optical applications. In addition, since free and trapped charge carriers of both positive and negative signs are known to form small polarons in LN, this material serves as an elegant and robust model system to study fundamental physical properties [1].

An electronic charge carrier becomes self-trapped when it is bound within the potential well produced by its displacements of the equilibrium positions of the atoms that surround it. The composite quasiparticle comprising a self-trapped electronic charge carrier taken together with the displaced

atomic equilibrium positions is termed polaron [1]. This name polaron was adopted in recognition of their prevalence in polar (i.e., ionic) materials.

Lithium niobate is a perovskite-like oxide ferroelectric with especially displaceable ions [2,3]. The dependence of the energy of an electronic carrier on displacements of surrounding atoms produces both long-range and short-range electron–phonon interactions. The long-range electron–phonon interaction results from the Coulomb energy of an electronic carrier depending on displacements of distant ions. It is proportional to $(1/\epsilon_\infty - 1/\epsilon_0)$, where ϵ_0 and ϵ_∞ respectively designate a material's static and high-frequency constant. Values of this parameter in LN ($\epsilon_0 = 30 - 80$, $\epsilon_\infty = 5.5$ [4]) are comparable to those of other ionic materials (e.g., alkali halides) whose charge carriers form polarons. Short-range electron–phonon interactions result from the energies and covalency of bonds between neighboring atoms changing with their separations. Short-range electron–lattice interactions as well as disorder foster the collapse of self-trapped electronic carriers to single sites thereby forming small polarons [1,5].

In addition to free small-polarons in LN [6], defects are sites for defect-related electron and hole polarons as well as bipolarons [7,8]. Small-polarons govern many of the linear and non-linear optical properties of LN [9–11] that include the bulk photovoltaic effect [12], green-induced infrared absorption (GRIIRA), optical damage and photoconductivity (PC) [8,11,13,14]. The transient broad-band small-polaron absorptions and index changes in LN [9,10] provide a clear link between small-polaron absorption and their hopping motion. For instance, the stretched-exponential relaxation of the transient absorption is attributed to small-polarons' hopping [15–17].

Small polarons exhibit distinctive optical and electronic transport properties [1]. In particular, phonon-broadened absorption bands result from photon-assisted inter-site transfers of small-polarons' self-trapped electronic carriers. In addition, small polarons generally move with extremely low mobilities via phonon-assisted hopping. A small-polaron absorption band disappears as its small polarons are eliminated by their recombination with oppositely charged carriers. Recombination is facilitated by both photon-assisted and phonon-assisted hopping. In the former case, increasing the intensity of absorption within a small-polaron band fosters its elimination. In this manner, small-polaron absorptions are bleached. In the latter case, increasing temperature fosters disappearance of small-polaron absorptions.

Essential features of a small-polaron's phonon-assisted hopping are well established [1]. Self-trapped electronic carriers usually move fast enough to adiabatically adjust to the relatively slow vibrations of atoms. Adiabatic small-polaron hopping has been addressed at high enough temperatures for atoms' vibrations to be classical. The small-polaron jump rate is then Arrhenius both for uncorrelated hops [18,19] and when the slow transfer of vibrational energy between atoms causes hops to occur in flurries with enhanced pre-exponential factors [1,20,21]. Nonetheless, for computational simplicity, almost all calculations of phonon-assisted hopping are performed in the non-adiabatic limit in which an electronic carrier's inter-site motion is assumed to be arbitrarily slow. In particular, the elemental non-adiabatic small-polaron jump rate has been calculated for its self-trapped carrier interacting with acoustic [22], optical [23] and both acoustic and optical phonons [24].

All studies of small-polaron hopping report three distinct temperature regimes [1]. At the highest temperatures, atoms' vibrations are classical with a self-trapped carrier moving between initial and final sites when its electronic energy at these sites become coincident with each other. The jump rate's primary temperature dependence is then Arrhenius and independent of phonon energies: $\propto \exp[-(4E_a + \Delta)^2/16E_a k_B T]$, where Δ denotes the energy difference between final and initial sites with E_a being the activation energy for equivalent sites, $\Delta = 0$. At the lowest temperatures, a self-trapped carrier hops when atoms quantum-mechanically tunnel between the configurations they assume when the self-trapped carrier occupies initial and final sites. The jump rate's primary temperature dependence is then also Arrhenius and independent of phonon energies: $\propto \exp[-(\Delta + |\Delta|)/2k_B T]$. Then a hop upward in energy, $\Delta > 0$, is Arrhenius, $\propto \exp(-\Delta/k_B T)$, while a

hop downward in energy, $\Delta < 0$, is temperature independent. Distinctively, the small-polaron jump rate between these high-temperature and low-temperature limits is non-Arrhenius and dependent on phonon energies. The primary temperature dependence of the small polaron jump rate is $\propto \exp[-(4E_a/\hbar\omega)\tanh(\hbar\omega/4k_BT)]\exp(-\Delta/2k_BT)$ for $|\Delta| \ll 4E_a$, where $\hbar\omega$ represents the characteristic phonon energy. Thus, measuring the temperature dependence in the high-temperature and intermediate regimes provides an estimate of this characteristic phonon energy. The reasonableness of this estimate tests the small-polaron approach.

Sufficiently separated oppositely charged small polarons will experience a mutual Coulomb attraction [1]. Recombination between oppositely charged small polarons can occur once a series of small-polaron hops enables them to move close enough to one another. These hops will tend to be downward in energy, $\Delta < 0$, since small-polaron jump rates are proportional to $\exp(-\Delta/2k_BT)$. The rate-limiting hop, the slowest of this sequence, occurs at its beginning where $|\Delta|$ tends to be smallest. Since the oppositely charged small polarons generated by our experiment's pump will have a distribution of initial separations, their recombination will be characterized by a distribution of recombination times. Thus, as observed [15], the time-dependent relaxation of the pump-induced transient absorption will be a stretched exponential.

We utilize a two-photon pump to produce electron and hole small-polarons whose recombination is then monitored by their absorption's temporal decay. To generate free small-polarons, we study an LN crystal that was congruently grown from a melt with 6.5 % Mg since it contains a negligible concentration of antisite defects. Our optical excitation then primarily produces free Nb^{4+} n-type small polarons and O^-–V_{Li} sites, p-type polarons bound to lithium vacancies [25,26]. We thereby avoid the profusion of other types of polaron states that occur in materials such as Fe:LN [17,27]. The transient near infra-red absorption in LN is primarily due to small polarons [6,28]. Other optical phenomena are also associated with self-trapped charge carriers and excitons [29–33]

We explore the transient absorption from 10^{-7} to 10^5 s for temperatures between 45 K and 225 K. A simple model enables us to relate the observed decay rate of the absorption to the temperature-dependent small-polaron jump rate. Analysis of the small-polaron jump rate through the observed temperature range yields plausible estimates of the activation energy for small-polaron hopping and distinctively, the characteristic atomic-vibration frequency.

2. Methods

The lithium niobate sample (thickness d = 2 mm, Mg-doping of 6.5 mol% in the melt, z-cut) was grown, cut and polished by Kovács et al. at the WIGNER Research Centre for Physics, Budapest. The crystal was mounted in a closed-cycle cryostat which operates between 40 K and room temperature.

Optical windows on the cryostat enable nanosecond-pump and continuous-wave-probe measurements for probing small-polarons' transient absorption (TA). Small polarons were generated in Mg:LN via two-photon absorption from an ordinarily polarized, frequency-doubled Nd:YAG pulse laser ($\lambda_p = 532$ nm, $\tau_{FWHM} = 8$ ns, $I_p \approx 170$ MW/cm^2). Transmitted polarized light of a continuous wave probe laser ($\lambda = 785$ nm) was split and detected (1) by a Si-PIN photo diode connected to a fast digital storage oscilloscope and (2) by a photometer. Thus, the TA signal was recorded (1) in a time range from nanoseconds up to five seconds and (2) in a time range from one second up to several thousands of seconds, respectively. The power of the probe laser was kept below 1 mW to minimize its effect on the transient absorption. For this purpose, a fast electronic shutter was also introduced into the probe beam's path so that the transient absorption at long times was only affected intermittently. The transient absorption $\alpha_{li}(\lambda, t)$ is determined from the ratio of the intensity of the transmitted probe light after the pulse was applied $I(\lambda, t)$ to that prior to the pulse event $I(\lambda, t \leq 0)$, giving: $\alpha_{li}(\lambda, t) = -(1/d)\ln[I(\lambda, t)/I(\lambda, t \leq 0)]$.

3. Decay of Photo-Induced Absorption

Figure 1 shows the normalized temperature-dependent results of transient absorption measurements at the probe wavelength $\lambda = 785$ nm for Mg:LN. Obviously, these data are not well described as simple temporal decays, $\exp[-(t/\tau)]$. However, our data are well fitted with the two temperature-dependent parameters [$\tau(T)$ and $\beta(T)$] of Kohlrausch–Williams–Watts (KWW) stretched-exponentials, $\exp[-(t/\tau)^{\beta}]$. The red curve accompanying the lowest-temperature data shows such a fit. The red curve accompanying the highest-temperature data illustrates that the fitting result is only slightly improved upon employing six adjustable parameters of a sum of two KWW stretched exponentials, $\alpha_{\mathrm{li},0}(1-f)\exp[-(t/\tau_1)^{\beta_1}] + \alpha_{\mathrm{li},0} f \exp[-(t/\tau_2)^{\beta_2}]$. We note that we used the fit parameter for the starting amplitude $\alpha_{\mathrm{li},0}$ to account for the elevation of the measured data above the value 1, that was caused by the noise in the experimental data. We therefore illustrate our results in terms of a single KWW stretched exponential with its two temperature dependent parameters, $\tau(T)$ and $\beta(T)$.

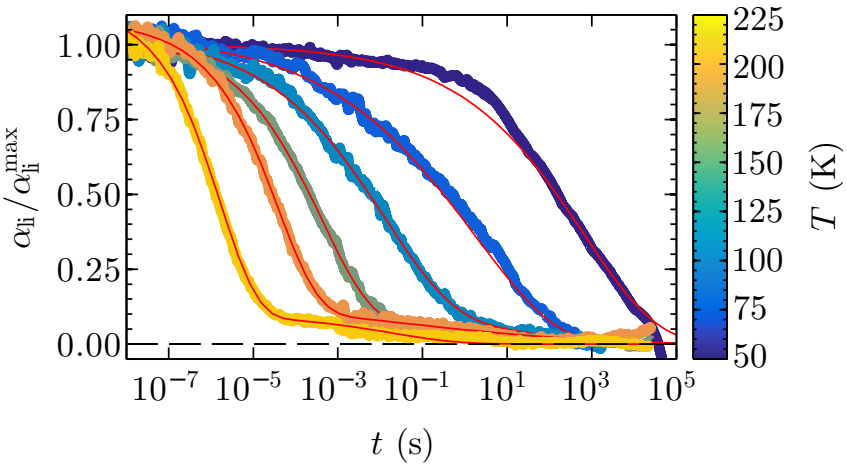

Figure 1. Normalized photo-absorptions at a wavelength of 785 nm of 6.5 mol% Mg:LN are plotted versus decay time for representative temperatures between 50 K and 225 K. The solid red curves show fits using a single Kohlrausch–Williams–Watts (KWW) stretched-exponential for $T < 100$ K and the sum of two KWW functions for $T > 100$ K, respectively.

KWW stretched-exponentials are phenomenological representations of processes with distributions of relaxation times. The mean relaxation time for a KWW stretched exponential is $\langle\tau(T)\rangle \equiv \tau(T)\Gamma\{[1/\beta(T)]+1\}$, where Γ denotes the mathematical gamma function. $\langle\tau(T)\rangle$ is found from the values of $\tau(T)$ and $\beta(T)$ obtained from stretched-exponential fits to our transient-absorption data.

The resulting values of $1/\langle\tau(T)\rangle$ plotted against reciprocal temperature in units of 1000/T are the experimental points shown in Figure 2. Distinctively, the photo-induced decay rate $1/\langle\tau(T)\rangle$ appears Arrhenius above 100 K and becomes non-Arrhenius below 100 K.

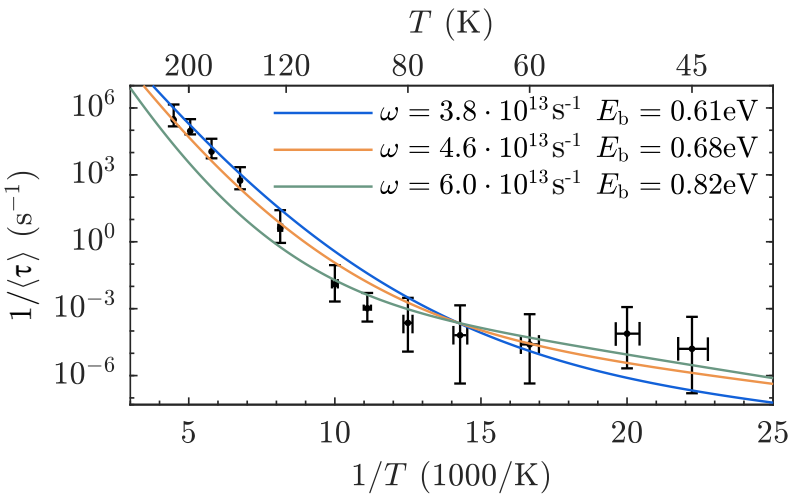

Figure 2. The temperature dependence of the inverse mean decay time of photo-induced absorption in Mg:LN is compared to the small-polaron hopping and recombination rate.

4. Small-Polaron Recombination and Phonon-Assisted Hopping

Well-separated oppositely charged small polarons attract each other through their mutual Coulomb attraction, $e^2/\epsilon_0 s$ when separated by distance s. Oppositely charged small polarons only recombine once they are close enough to one another to overlap significantly. Small polarons move toward recombination via a series of phonon-assisted hops. The rate for each phonon-assisted jump increases as the energy of its final state falls increasingly below that of its initial state except when this energy disparity is exceptionally large [1,22–24]. Thus, the recombination of well-separated oppositely charged small polarons tends to occur via a series of jumps in which each hop is progressively faster. The rate-limiting jump is the initial hop of this series, a jump with minimal energy disparity. The recombination rate of oppositely charged small polarons therefore is determined by the hop between sites of nearly equal energy.

A phonon-assisted hop occurs when an electronic carrier transfers between sites in response to atoms assuming favorable configurations [1]. A hop is termed non-adiabatic when the inter-site transfer energy of the electronic charge carrier is so small that it rarely avails itself of the opportunity to move [18,19]. Alternatively, adiabatic hopping occurs when the electronic carriers are able to adjust to changing atomic configurations. Small-polaron hopping is generally adiabatic [1]. Nonetheless, phonon-assisted jump rates are usually computed for the non-adiabatic limit, where they are perturbative to lowest-order in the hop's electronic transfer-energy.

The non-adiabatic small-polaron jump rate has been calculated exactly for the Holstein Molecular-Crystal-Model (MCM), where the electronic carrier is assumed to interact with a single vibrational mode of frequency ω, only [23]. To enable small-polaron formation in this idealized model, its small-polaron binding energy E_b is taken to exceed both the phonon energy $\hbar\omega$ and the inter-site electronic transfer energy J. An approximate formula for the adiabatic small-polaron jump rate is obtained at all but very low temperatures when dividing this non-adiabatic rate by the high-temperature probability of the electronic carrier transferring in response to an appropriate atomic configuration [1,19]. In particular, the approximate formula for the adiabatic rate for a hop between equivalent sites is found by dividing the right-hand-side of Equation (59) of Ref. [23] by $J^2/(\hbar\omega/2\pi)(2E_b k_B T/\pi)^{1/2}$:

$$R_{ad} = \sqrt{\frac{E_b k_B T}{\pi\hbar^2}} \exp\left[-\left(\frac{2E_b}{\hbar\omega}\right)\coth\left(\frac{\hbar\omega}{2k_B T}\right)\right]\left\{I_0\left[\left(\frac{2E_b}{\hbar\omega}\right)\operatorname{csch}\left(\frac{\hbar\omega}{2k_B T}\right)\right]-1\right\}. \quad (1)$$

where $I_0(x)$ denotes the zeroth-order modified Bessel function. At high and intermediate temperatures relative to $\hbar\omega$, this expression becomes

$$R_{\mathrm{ad}} \cong \left(\frac{\omega}{2\pi}\right) \exp\left[\left(\frac{2E_{\mathrm{b}}}{\hbar\omega}\right) \tanh\left(\frac{\hbar\omega}{4k_{\mathrm{B}}T}\right)\right]. \tag{2}$$

Distinctively, the Arrhenius behavior with activation energy $E_{\mathrm{b}}/2$ progressively disappears as $k_{\mathrm{B}}T$ is lowered relative to $\hbar\omega/4$. In other words, as shown in Figure 3, the activation energy progressively shrinks from $E_{\mathrm{b}}/2$ as the temperature is reduced.

Beyond the simple MCM, a small-polaron's phonon-assisted hop is primarily associated with movements of the atoms in the immediate vicinity of its self-trapped electronic carrier [1]. As such, a small-polaron hop generally involves interactions with short-wavelength phonons from both acoustic and optic vibration modes. The activation energy for an Arrhenius small-polaron jump is the sum of contributions from these modes. The pre-exponential factor of the adiabatic jump rate of Equation (2) is then the square-root of the sum of the squares of these zone edge phonons weighted by their relative contributions to the jump's activation energy [19].

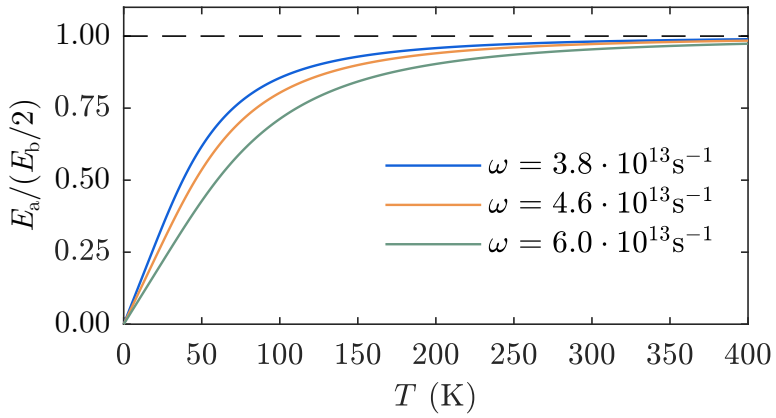

Figure 3. Normalized small-polaron hopping activation energy E_{a} over $E_{\mathrm{b}}/2$ as a function of temperature. Note the different slopes and absolute values at different phonon frequencies, ω, when lowering the temperature.

5. Combining the Decay of Lithium Niobate's Induced Absorption with Small-Polaron Recombination

We ascribe the observed photo-induced absorption mainly to photo-generated Nb^{4+} n-type free small polarons. The decay of this photo-induced absorption is attributed to their recombination with p-type small polarons that are bound to lithium vacancies, $O^{-}-V_{Li}$. This attribution is supported by evidence of only negligible Fe and Nb_{Li} contamination in these crystals [17]. Indeed, room-temperature transient absorption measurements on a series of Mg-doped and nominally pure LN samples by Conradi et al. [26] also concluded that the primary signal at 785 nm stems from Nb^{4+} free small polarons. Furthermore, subsequent work only found a secondary relatively weak and slow decay that most likely results from the recombination of self-trapped excitons pinned at various defects [29,31]. As shown in Figure 1, a single KWW function provides a satisfactory fit to our low-temperature data.

Distinctively, we measure the decay of the photo-induced absorption in Mg:LN over a wide temperature range. As a result, we observe the shift from Arrhenius behavior at highest temperatures to a relatively weak temperature-dependence at lowest temperatures. This fundamental feature of small-polarons' hopping is sensitive to the phonon energies with which their self-trapped electrons interact [1,22–24]. As shown in Figure 2, the mean decay time of the photo-induced absorption is well fitted by our model for small-polaron recombination. Best fit's are obtained for $E_{\mathrm{b}} = 0.68$ eV and $\omega = 4.6 \times 10^{13}$ s^{-1}. Both of these values are typical of small-polaron hopping.

6. Discussion

Polarons are generally characterized by broad asymmetric absorption bands. These absorptions arise from exciting polarons' self-trapped electronic carriers from the potential wells that bind them [1,34]. As shown in Figures 5 and 6 of Ref. [34], small-polaron absorption bands tend to be higher on the low-frequency side of their peaks. By contrast, large-polaron absorptions tend to be higher on the high-frequency side of their peaks [34]. This distinction can be used to differentiate between small-polaron and large-polaron absorption bands. As illustrated in Figure 7 of Ref. [23], the peak of the small-polaron absorption in the MCM occurs at $2E_b$, twice the small-polaron binding energy. This figure shows that the absorption becomes broader and less symmetric with increasing temperature. An early calculation of a small-polaron absorption band [35] did not adequately describe its width and inherent asymmetry.

In the non-adiabatic limit of the MCM, the activation energy for Arrhenius small-polaron hopping E_a is simply half the small-polaron binding energy E_b. However, the MCM only envisions a short-range component of the electron–phonon interaction. As noted in this paper's introduction, LN is an ionic material with a significant long-range component of its electron–phonon interaction. As the long-range component of the electron–phonon interaction increases, E_a decreases as a fraction of the small-polaron binding energy [1]. Furthermore, the small-polaron hopping activation energy decreases upon progressing from the non-adiabatic limit into the adiabatic regime [1,18]. Thus, a small-polaron's binding energy E_b will tend to be somewhat larger than twice the activation energy of its high-temperature Arrhenius hopping E_a.

A polaron becomes small when its self-trapped electronic carrier collapses to a single site, e.g., a single Nb cation in LN. Its self-trapped electronic carrier then hops between adjacent sites by primarily interacting with short-wavelength phonons. The characteristic phonon frequency for small-polaron hopping will then be comparable to those of these short-wavelength modes. In LN these modes have wavenumbers of about 250 cm^{-1} [36–39]. The inverse of the frequencies of these modes also corresponds to the time determined for atoms to shift their equilibrium positions in response to the addition of a severely localized electronic charge carrier [40,41]. Thus, the frequencies of these short-wavelength phonons are comparable to what we measure to be the characteristic phonon frequency associated with n-type small-polaron hopping in LN, $\omega = 4.6 \times 10^{13}$ s^{-1}.

7. Summary

In summary, we measured the temporal decay of the photo-induced absorption of Mg:LN from 45 K to 225 K. The time dependencies of decays of the induced absorption at 785 nm fit well with the phenomenological Kohlrausch–Williams–Watts (KWW) stretched-exponentials, $\exp[-(t/\tau)^{\beta}]$. The effective decay rate, the inverse of the mean decay time of each KWW curve, a function of τ and β, is a function of temperature. At the highest temperatures, the decay rate for the photo-induced absorption manifests an Arrhenius temperature dependence. This temperature dependence weakens and becomes non-Arrhenius as the temperature is lowered.

These decays are ascribed to the hopping of Nb^{4+} n-type small polarons leading to their eventual recombination with O^{-} p-type small polarons bound to Li vacancies. The n-type and p-type small polarons are attracted to one another by their mutual Coulomb attraction reduced by the static dielectric constant of LN. We model this hopping sequence as a series of jumps that are increasingly downward in energy. The rate-limiting step in this sequence of small-polaron hops, its slowest jump, is then its first step since its energy disparity is smallest. We take the energy disparity of well-separated oppositely charged small polarons to be minimal. As such, we compare the adiabatic jump rate of small polarons between sites of equal energy with the inverse of the mean decay time for KWW decays.

The rate for adiabatic small-polaron hops between equivalent sites is Arrhenius at high temperatures. As the temperature is reduced the temperature dependence of this adiabatic small-polaron jump rate weakens as it becomes non-Arrhenius [1,22–24]. The transition between these two behaviors occurs at the temperature corresponding to a significant fraction of that

characterizing the principal phonons with which a small-polaron's self-trapped electronic carrier interacts. This feature yields a more precise value for the characteristic phonon frequency than can be obtained from only fitting data from the high-temperature Arrhenius region. Fitting the decay rate of photo-induced decay in Mg:LN to the adiabatic small-polaron jump rate between equivalent states yields reasonable values of the small-polaron binding energy and the characteristic frequency of the phonons with which its self-trapped electron interacts: $E_b = 0.68\,\text{eV}$ and $\omega = 4.6 \times 10^{13}\,\text{s}^{-1}$.

Author Contributions: Conceptualization, S.M. and M.I.; Methodology, S.M. and T.N.; Software, S.M. and A.K.; Validation, S.M., A.K. and L.V.; Formal Analysis, S.M., A.K. and T.N.; Investigation, S.M., A.K. and L.V.; Writing—Original Draft Preparation, S.M., A.K., M.I. and D.E.; Writing—Review & Editing, S.M., A.K., L.V., M.I., L.M.E. and D.E.; Visualization, S.M. and A.K.; Project Administration, M.I.; Funding Acquisition, M.I. and L.M.E. All authors have read and agreed to the published version of the manuscript.

Funding: This research was funded by the Deutsche Forschungsgemeinschaft, DFG, grant numbers: IM 37/11-1, INST 190/137-1 FUGG, and INST 190/165-1 (S.M., A.K., L.V., M.I.) and the Bundesministerium für Bildung und Forschung, BMBF, grant number 05K16ODA (T.N.) and through the Center of Excellence—Complexity and Topology in Quantum Matter (ct.qmat) (L.M.E.). Support by Deutsche Forschungsgemeinschaft (DFG) and Open Access Publishing Fund of Osnabrück University is gratefully acknowledged.

Acknowledgments: The authors thank L. Kovács and coworkers at the Wigner Research Centre for Physics, Budapest, for crystal preparation.

Conflicts of Interest: The authors declare no conflict of interest.

References

1. Emin, D. *Polarons*; Cambridge University Press: Cambridge, UK, 2012.
2. Freytag, F.; Corradi, G.; Imlau, M. Atomic insight to lattice distortions caused by carrier self-trapping in oxide materials. *Sci. Rep.* **2016**, *6*, 36929. [CrossRef] [PubMed]
3. Sanson, A.; Zaltron, A.; Argiolas, N.; Sada, C.; Bazzan, M.; Schmidt, W.G.; Sanna, S. Polaronic deformation at the $Fe^{2+/3+}$ impurity site in Fe:$LiNbO_3$ crystals. *Phys. Rev. B* **2015**, *91*, 094109. [CrossRef]
4. Weis, R.S.; Gaylord, T.K. Lithium niobate: Summary of physical properties and crystal structure. *Appl. Phys. A* **1985**, *37*, 191–203. [CrossRef]
5. Emin, D.; Holstein, T. Adiabatic Theory of an Electron in a Deformable Continuum. *Phys. Rev. Lett.* **1976**, *36*, 323–326. [CrossRef]
6. Faust, B.; Müller, H.; Schirmer, O.F. Free small polarons in $LiNbO_3$. *Ferroelectrics* **1994**, *153*, 297–302. [CrossRef]
7. Schirmer, O.F. O^- bound small polarons in oxide materials. *J. Phys. Condens. Matter* **2006**, *18*, R667–R704. [CrossRef]
8. Schirmer, O.F.; Imlau, M.; Merschjann, C.; Schoke, B. Electron small polarons and bipolarons in $LiNbO_3$. *J. Phys. Condens. Matter* **2009**, *21*, 123201. [CrossRef]
9. Imlau, M.; Brüning, H.; Schoke, B.; Hardt, R.-S.; Conradi, D.; Merschjann, C. Hologram recording via spatial density modulation of $Nb_{Li}^{4+/5+}$ antisites in lithium niobate. *Opt. Express* **2011**, *19*, 15322–15338. [CrossRef]
10. Brüning, H.; Dieckmann, V.; Schoke, B.; Voit, K.-M.; Imlau, M.; Corradi, G.; Merschjann, C. Small-polaron based holograms in $LiNbO_3$ in the visible spectrum. *Opt. Express* **2012**, *20*, 13326–13336. [CrossRef]
11. Imlau, M.; Badorreck, H.; Merschjann, C. Optical nonlinearities of small polarons in lithium niobate. *Appl. Phys. Rev.* **2015**, *2*, 040606. [CrossRef]
12. Schirmer, O.F.; Imlau, M.; Merschjann, C. Bulk photovoltaic effect of $LiNbO_3$:Fe and its small-polaron-based microscopic interpretation. *Phys. Rev. B* **2011**, *83*, 165106. [CrossRef]
13. Furukawa, Y.; Kitamura, K.; Alexandrovski, A.; Route, R.K.; Fejer, M.M.; Foulon, G. Green-induced infrared absorption in MgO doped $LiNbO_3$. *Appl. Phys. Lett.* **2001**, *78*, 1970–1972. [CrossRef]
14. Hirohashi, J.; Pasiskevicius, V.; Wang, S.; Laurell, F. Picosecond blue-light-induced infrared absorption in single-domain and periodically poled ferroelectrics. *J. Appl. Phys.* **2007**, *101*, 033105. [CrossRef]
15. Berben, D.; Buse, K.; Wevering, S.; Herth, P.; Imlau, M.; Woike, T. Lifetime of small polarons in iron-doped lithium niobate crystals. *J. Appl. Phys.* **2000**, *87*, 1034–1041. [CrossRef]
16. Mhaouech, I.; Guilbert, L. Temperature dependence of small polaron population decays in iron-doped lithium niobate by Monte Carlo simulations. *Solid State Sci.* **2016**, *60*, 28–36. [CrossRef]

17. Vittadello, L.; Bazzan, M.; Messerschmidt, S.; Imlau, M. Small Polaron Hopping in Fe:$LiNbO_3$ as a Function of Temperature and Composition. *Crystals* **2018**, *8*, 294. [CrossRef]
18. Emin, D.; Holstein, T. Studies of small polaron motion IV: Adiabatic theory of the Hall Effect. *Ann. Phys.* **1969**, *53*, 439–520. [CrossRef]
19. Emin, D. Semiclassical small-polaron hopping in a generalized molecular-crystal model. *Phys. Rev. B* **1991**, *43*, 11720. [CrossRef]
20. Emin, D. Generalized adiabatic polaron hopping: Meyer-Neldel compensation and Poole-Frenkel behavior. *Phys. Rev. Lett.* **2008**, *100*, 166602. [CrossRef]
21. Emin, D. Theory of Meyer–Neldel compensation for adiabatic charge transfer. *Monatshefte Für Chem.- Mon.* **2012**, *144*, 3–10. [CrossRef]
22. Emin, D. Phonon-assisted jump rate in noncrystalline solids. *Phys. Rev. Lett.* **1974**, *32*, 303–307. [CrossRef]
23. Emin, D. Phonon-assisted transition rates I. Optical-phonon-assisted hopping in solids. *Adv. Phys.* **1975**, *24*, 305–348. [CrossRef]
24. Gorham-Bergeron, E.; Emin, D. Phonon-assisted hopping due to interaction with both acoustical and optical phonons. *Phys. Rev. B* **1977**, *15*, 3667–3680. [CrossRef]
25. Volk, T.; Wöhlecke, M. *Lithium Niobate*; Springer GmbH: Berlin/Heidelberg, Germany, 2008.
26. Conradi, D.; Merschjann, C.; Schoke, B.; Imlau, M.; Corradi, G.; Polgár, K. Influence of Mg doping on the behaviour of polaronic light-induced absorption in $LiNbO_3$. *Phys. Stat. Sol. (RRL)* **2008**, *2*, 284–286. [CrossRef]
27. Guilbert, L.; Vittadello, L.; Bazzan, M.; Mhaouech, I.; Messerschmidt, S.; Imlau, M. The elusive role of Nb_{Li} bound polaron energy in hopping charge transport in Fe:$LiNbO_3$. *J. Phys. Condens. Matter* **2018**, *30*, 125701. [CrossRef]
28. Merschjann, C.; Schoke, B.; Conradi, D.; Imlau, M.; Corradi, G.; Polgár, K. Absorption cross sections and number densities of electron and hole polarons in congruently melting $LiNbO_3$. *J. Phys. Condens. Matter* **2008**, *21*, 015906. [CrossRef]
29. Messerschmidt, S.; Krampf, A.; Freytag, F.; Imlau, M.; Vittadello, L.; Bazzan, M.; Corradi, G. The role of self-trapped excitons in polaronic recombination processes in lithium niobate. *J. Phys. Condens. Matter* **2019**, *31*, 065701. [CrossRef]
30. Freytag, F.; Booker, P.; Corradi, G.; Messerschmidt, S.; Krampf, A.; Imlau, M. Picosecond near-to-mid-infrared absorption of pulse-injected small polarons in magnesium doped lithium niobate. *Opt. Mater. Express* **2018**, *8*, 1505. [CrossRef]
31. Messerschmidt, S.; Bourdon, B.; Brinkmann, D.; Krampf, A.; Vittadello, L.; Imlau, M. Pulse-induced transient blue absorption related with long-lived excitonic states in iron-doped lithium niobate. *Opt. Mater. Express* **2019**, *9*, 2748. [CrossRef]
32. Corradi, G.; Krampf, A.; Messerschmidt, S.; Vittadello, L.; Imlau, M. Excitonic hopping-pinning scenarios in lithium niobate based on atomistic models: Different kinds of stretched exponential kinetics in the same system. *J. Phys. Condens. Matter* **2020**, *32*, 413005. [CrossRef]
33. Krampf, A.; Messerschmidt, S.; Imlau, M. Superposed picosecond luminescence kinetics in lithium niobate revealed by means of broadband fs-fluorescence upconversion spectroscopy. *Sci. Rep.* **2020**, *10*, 11397. [CrossRef]
34. Emin, D. Optical properties of large and small polarons and bipolarons. *Phys. Rev. B* **1993**, *48*, 13691–13702. [CrossRef] [PubMed]
35. Reik, H.G.; Heese, D. Frequency dependence of the electrical conductivity of small polarons for high and low temperatures. *J. Phys. Chem. Solids* **1967**, *28*, 581–596. [CrossRef]
36. Caciuc, V.; Postnikov, A.V.; Borstel, G. Ab initiostructure and zone-center phonons in $LiNbO_3$. *Phys. Rev. B* **2000**, *61*, 8806–8813. [CrossRef]
37. Fontana, M.D.; Bourson, P. Microstructure and defects probed by Raman spectroscopy in lithium niobate crystals and devices. *Appl. Phys. Rev.* **2015**, *2*, 040602. [CrossRef]
38. Sanna, S.; Neufeld, S.; Rüsing, M.; Berth, G.; Zrenner, A.; Schmidt, W.G. Raman scattering efficiency in $LiTaO_3$ and $LiNbO_3$ crystals. *Phys. Rev. B* **2015**, *91*, 224302. [CrossRef]
39. Xin, F.; Zhai, Z.; Wang, X.; Kong, Y.; Xu, J.; Zhang, G. Threshold behavior of the Einstein oscillator, electron-phonon interaction, band-edge absorption, and small hole polarons in $LiNbO_3$:Mg crystals. *Phys. Rev. B* **2012**, *86*, 165132. [CrossRef]

40. Badorreck, H.; Nolte, S.; Freytag, F.; Bäune, P.; Dieckmann, V.; Imlau, M. Scanning nonlinear absorption in lithium niobate over the time regime of small polaron formation. *Opt. Mater. Express* **2015**, *5*, 2729. [CrossRef]
41. Sasamoto, S.; Hirohashi, J.; Ashihara, S. Polaron dynamics in lithium niobate upon femtosecond pulse irradiation: Influence of magnesium doping and stoichiometry control. *J. Appl. Phys.* **2009**, *105*, 083102. [CrossRef]